Analytical solution of the Poisson-Nernst-Planck equations for an electrochemical system close to electroneutrality

M. Pabst

Citation: The Journal of Chemical Physics **140**, 224113 (2014); doi: 10.1063/1.4881599
View online: http://dx.doi.org/10.1063/1.4881599
View Table of Contents: http://scitation.aip.org/content/aip/journal/jcp/140/22?ver=pdfcov
Published by the AIP Publishing

Analytical solution of the Poisson-Nernst-Planck equations for an electrochemical system close to electroneutrality

M. Pabst[a)]
Institute of Complex Systems (ICS-8), Forschungszentrum Jülich, 52425 Jülich, Germany

(Received 20 November 2013; accepted 23 May 2014; published online 13 June 2014)

Single charge densities and the potential are used to describe models of electrochemical systems. These quantities can be calculated by solving a system of time dependent nonlinear coupled partial differential equations, the Poisson-Nernst-Planck equations. Assuming small deviations from the electroneutral equilibrium, the linearized and decoupled equations are solved for a radial symmetric geometry, which represents the interface between a cell and a sensor device. The densities and the potential are expressed by Fourier-Bessels series. The system considered has a ratio between the Debye-length and its geometric dimension on the order of 10^{-4} so the Fourier-Bessel series can be approximated by elementary functions. The time development of the system is characterized by two time constants, τ_c and τ_g. The constant τ_c describes the approach to the stationary state of the total charge and the potential. τ_c is several orders of magnitude smaller than the geometry-dependent constant τ_g, which is on the order of 10 ms characterizing the transition to the stationary state of the single ion densities. © *2014 AIP Publishing LLC*. [http://dx.doi.org/10.1063/1.4881599]

I. INTRODUCTION

Systems with mass and charge transport in the presence of electric fields and diffusion are often described mathematically by the Poisson-Nernst-Planck (PNP) equation system. Therefore, the PNP equations have a wide range of application in physics, chemistry, biology, and engineering sciences. In that sense, e.g., the drift diffusion equations used for electrons and holes in semiconductor devices,[1,2] or the transport equations of ions in electrolytes,[3] are PNP equations. In biophysics, the PNP equations are often used to describe the electrodiffusion of ions in ion channels of the cell membrane.[4]

The PNP equation system consists of nonlinear coupled partial differential equations. It describes the potential, the ion densities, and the ion flux in a selfconsistent way; that is, the electric fields generated by the ions themselves are included. Due to the nonlinearity and the complexity of the differential equations numerical methods are usually applied to solve the PNP equations.[5–9]

In certain cases, analytical solutions have been found. Time independent and one-dimensional cases have been solved in Refs. 10–12. Due to the nonlinearity the solutions can be expressed by Jacobian elliptical functions.[11,12] An analysis of the time dependent single species system is shown in Ref. 13. Laplace transformation is applied to find approximate solutions for large voltages for a symmetric binary electrolyte between two parallel blocking electrodes, as shown in Ref. 3. For the same situation, but with a small external DC voltage, an exact analytical solution is obtained for the linearized PNP equations in Ref. 14.

In Sec. II, the PNP equations are linearized and decoupled. The charge densities of the different ion species are represented as a linear superposition of the total charge density and the total ion density of the electrolytic system. In Sec. III, the equations are solved for a radial symmetric system, which represents a cell-sensor interface.

II. THE POISSON-NERNST-PLANCK EQUATIONS

The PNP equation system couples the continuity equations, the Nernst-Planck equations and the Poisson equation. It describes the electrochemistry of a system with different ion species. For each ion, indexed by i, let $\rho_i(\boldsymbol{r}, t)$ and $\boldsymbol{j}_i(\boldsymbol{r}, t)$ represent the electrical charge densities and the electrical current densities, respectively. The densities are functions of the position $\boldsymbol{r}$ and the time t. If λ_i defines the source rate of the different ions, the continuity equations are given by

$$\nabla \cdot \mathbf{j}_i(\mathbf{r}, t) + \frac{\partial \rho_i(\mathbf{r}, t)}{\partial t} = \lambda_i. \tag{1}$$

In the most general case, λ_i is a function of $\boldsymbol{r}$ and t. However, here it is restricted to a constant value not dependent on position and time.

Current densities, charge densities, and the electrical potential $\psi(\boldsymbol{r}, t)$ are coupled via the Nernst-Planck equations

$$\mathbf{j}_i(\mathbf{r}, t) = -D_i\left(\nabla \rho_i(\mathbf{r}, t) + \frac{z_i e}{k_B T}\rho_i(\mathbf{r}, t)\nabla\psi(\mathbf{r}, t)\right) \tag{2}$$

with the diffusion coefficients D_i and the electric charge number z_i of ion i. The quantities e, k_B, and T are the elementary charge, Boltzmann's constant, and temperature, respectively. The potential is coupled to the total charge density $\rho_{tot}(\boldsymbol{r}, t) = \Sigma\rho_i(\boldsymbol{r}, t)$ by the Poisson equation

$$\Delta\psi(\mathbf{r}, t) = -\frac{\rho_{tot}(\mathbf{r}, t)}{\epsilon_0\epsilon_r} \tag{3}$$

with the permittivities ϵ_0 and ϵ_r. For the following discussion, it is useful to introduce ion densities n_i by $n_i(\boldsymbol{r}, t) = \rho_i(\boldsymbol{r}, t)/(z_i e)$. In analogy to ρ_{tot}, the total ion density n_{tot}

a)Electronic mail: M.Pabst@fz-juelich.de

is given by the $n_{tot} = \Sigma n_i$. For the application discussed below, it is assumed that the diffusion of the different ions is characterized by a common diffusion coefficient D and that the charge number z_i is given either by +1 or −1. Thus, by summing over the index i and combining Eqs. (1)–(3) one obtains for ρ_{tot} and n_{tot} the two equations

$$\Delta\rho_{tot}(\boldsymbol{r},t) + \frac{e^2}{k_B T}\nabla\cdot[n_{tot}(\boldsymbol{r},t)\nabla\psi(\boldsymbol{r},t)] - \frac{1}{D}\frac{\partial\rho_{tot}(\boldsymbol{r},t)}{\partial t} = -\frac{\lambda_{tot}}{D}, \tag{4}$$

$$\Delta n_{tot}(\boldsymbol{r},t) + \frac{1}{k_B T}\nabla\cdot[\rho_{tot}(\boldsymbol{r},t)\nabla\psi(\boldsymbol{r},t)] - \frac{1}{D}\frac{\partial n_{tot}(\boldsymbol{r},t)}{\partial t} = -\frac{\zeta_{tot}}{D}, \tag{5}$$

with $\lambda_{tot} = \Sigma\lambda_i$ and $\zeta_{tot} = \Sigma\lambda_i/(z_i e)$.

For the last two equations, the following assumptions are made. First, to linearize the equations only small deviations of the charge densities from their constant equilibrium value $\rho_i(\boldsymbol{r},t) = \rho_i^e + \delta\rho_i(\boldsymbol{r},t)$ with $\delta\rho_i(\boldsymbol{r},t) \ll \rho_i^e$ are assumed. By defining $n_i^e = \rho_i^e/(z_i e)$ and $\delta n_i(\boldsymbol{r},t) = \delta\rho_i(\boldsymbol{r},t)/(z_i e)$ it follows that $n_i(\boldsymbol{r},t) = n_i^e + \delta n_i(\boldsymbol{r},t)$ with $\delta n_i(\boldsymbol{r},t) \ll n_i^e$. As a consequence, one has $\rho_{tot}(\boldsymbol{r},t) = \rho_{tot}^e + \delta\rho_{tot}(\boldsymbol{r},t)$ and $n_{tot}(\boldsymbol{r},t) = n_{tot}^e + \delta n_{tot}(\boldsymbol{r},t)$ with $\rho_{tot}^e = \Sigma\rho_i^e$, $n_{tot}^e = \Sigma n_i^e$, $\delta\rho_{tot}(\boldsymbol{r},t) = \Sigma\delta\rho_i(\boldsymbol{r},t)$, and $\delta n_{tot}(\boldsymbol{r},t) = \Sigma\delta n_i(\boldsymbol{r},t)$. It is clear that $\delta n_{tot}(\boldsymbol{r},t) \ll n_{tot}^e$ while a corresponding relation does not necessarily hold for the total charge density. Second, to decouple the equations, the equilibrium state should be electroneutral, which means that $\rho_{tot}^e = 0$ and at least two ion species of opposite charge must be present.

Applying these assumptions to Eqs. (4) and (5) one obtains an inhomogeneous Debye Falkenhagen equation[15] for $\rho_{tot}(r,t) = \delta\rho_{tot}(\boldsymbol{r},t)$

$$\Delta\delta\rho_{tot}(\boldsymbol{r},t) - \frac{1}{L_D^2}\delta\rho_{tot}(\boldsymbol{r},t)) - \frac{1}{D}\frac{\partial\delta\rho_{tot}(\boldsymbol{r},t)}{\partial t} = -\frac{\lambda_{tot}}{D} \tag{6}$$

with the Debye length L_D defined by

$$L_D = \sqrt{\frac{\epsilon_0\epsilon_r kT}{e^2 n_{tot}^e}}. \tag{7}$$

For $\delta n_{tot}(\boldsymbol{r},t)$, it follows from Eq. (5) an inhomogeneous diffusion equation

$$\Delta\delta n_{tot}(\boldsymbol{r},t) - \frac{1}{D}\frac{\partial\delta n_{tot}(\boldsymbol{r},t)}{\partial t} = -\frac{\zeta_{tot}}{D}. \tag{8}$$

Returning to the single charge densities, Eqs. (1)–(3), together with the stated assumptions, give

$$\Delta\delta\rho_i(\boldsymbol{r},t) - \frac{1}{D}\frac{\partial\delta\rho_i(\boldsymbol{r},t)}{\partial t} = -\frac{1}{L_D^2}\frac{n_i^e}{n_{tot}^e}\delta\rho_{tot}(\boldsymbol{r},t) - \frac{\lambda_{tot}}{D}. \tag{9}$$

To solve these equations, the following linear ansatz is made:

$$\delta\rho_i(\boldsymbol{r},t) = \alpha_i\delta n_{tot}(\boldsymbol{r},t) + \beta_i\delta\rho_{tot}(\boldsymbol{r},t). \tag{10}$$

The equation $\Sigma\delta\rho_i(\boldsymbol{r},t) = \delta\rho_{tot}(\boldsymbol{r},t)$ can be fulfilled with $\Sigma\alpha_i = 0$ and $\Sigma\beta_i = 1$.

By setting

$$\beta_i = \frac{n_i^e}{n_{tot}^e} \tag{11}$$

and

$$\alpha_i = \frac{1}{\zeta_{tot}}(\lambda_i - \lambda_{tot}\beta_i), \tag{12}$$

the ansatz of Eq. (10) is a solution of Eq. (9). The deviations $\delta\rho_i$ of single charge densities can be expressed by a linear superposition of δn_{tot} and $\delta\rho_{tot}$.

From Eq. (6) a differential equation for the potential $\psi(\boldsymbol{r},t)$ can be derived. Remembering that $\rho_{tot}(\boldsymbol{r},t) = \delta\rho_{tot}(\boldsymbol{r},t)$ and using Eq. (3) one obtains a fourth order differential equation for the potential

$$\Delta\left[\Delta\psi(\boldsymbol{r},t) - \frac{1}{L_D^2}\psi(\boldsymbol{r},t) - \frac{1}{D}\frac{\partial\psi(\boldsymbol{r},t)}{\partial t}\right] = \frac{\lambda_{tot}}{\epsilon_0\epsilon_r D}. \tag{13}$$

III. APPLICATION TO THE CELL-SENSOR INTERFACE

The method described is applied to the electrical description of a cell-sensor interface. The time dependent PNP equations are solved in polar coordinates. The time independent long term limit has already been discussed.[16]

A schematic picture of the cell-sensor interface is shown in Fig. 1. A human embryonic kidney cell (HEK EAG) is placed above the gate of a field-effect transistor (FET). The region to be discussed is the cleft between cell bottom and FET surface. The cleft is represented by a thin disk with a height h less than 100 nm and a radius R of about 15 μm, giving a ratio $h/R < 10^{-2}$.

By exciting the cell electrically at $t = 0$ the K^+ channels of the cell membrane open and the K^+ ions flow from inside of the cell into the surrounding electrolyte solution. While in the upper part of the cell the K^+ ions enter the surrounding electroneutral bath directly the ions at the bottom have to pass the cleft first before entering the bath. K^+ ions which enter the cleft will accumulate and increase the charge there. As a consequence, other ions of the electrolyte solution start to move. Positive ions will leave the cleft through the outer boundary of the disk moving into the surrounding electroneutral bath solution while negative ions will move in the opposite direction. Connected with this ion flux is a change of the total charge in

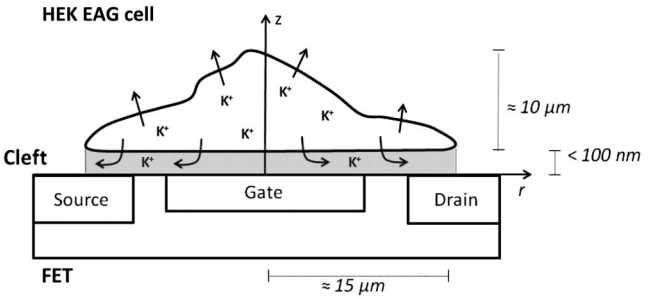

FIG. 1. A schematic picture of the cell-sensor interface. A HEK EAG cell is placed above a FET. The cleft between the bottom of the cell and the surface of the FET is represented by a thin disk with a height h less than 100 nm and a radius R of about 15 μm resulting in a ratio $h/R < 10^{-2}$. Please note that the given dimensions are not to scale.

the cleft that modifies the gate voltage of the attached FET. Thus, the flux of ions can be related to the FET signal.

Three ion species are considered for the electrolytic solution in the cleft: potassium (K^+), sodium (Na^+), and chloride (Cl^-). It is assumed that before the cell is excited electrically the ion concentrations ($i = K^+,\ Na^+,\ Cl^-$) inside the cleft are equal to the ion concentrations in the surrounding bath. Typical ion concentrations of the equilibrium are $c^e_{K^+} = 5$ mM, $c^e_{Na^+} = 140$ mM, $c^e_{Cl^-} = 145$ mM, and $c^e_{tot} = 290$ mM corresponding to the ion densities $n^e_{K^+} = 3.0 \times 10^{24}\ \mathrm{m}^{-3}$, $n^e_{Na^+} = 8.4 \times 10^{25}\ \mathrm{m}^{-3}$, $n^e_{Cl^-} = 8.7 \times 10^{25}\ \mathrm{m}^{-3}$, and $n^e_{tot} = 17.4 \times 10^{25}\ \mathrm{m}^{-3}$. With $\epsilon_r = 78$ one calculates for the Debye-length $L_D = 0.8$ nm at $T = 300$ K.

Unfortunately, the diffusion coefficients $D_{K^+} = 1.96 \times 10^{-9}\ \mathrm{m}^2\ \mathrm{s}^{-1}$, $D_{Na^+} = 1.33 \times 10^{-9}\ \mathrm{m}^2\ \mathrm{s}^{-1}$, and $D_{Cl^-} = 2.03 \times 10^{-9}\ \mathrm{m}^2\ \mathrm{s}^{-1}$ are not equal. As seen below, the diffusion coefficients enter the expressions for the time constants, which differ by several orders of magnitude. Therefore, the difference of the diffusion coefficients is of higher order and does not effect the conclusions made below.

When K^+ ions enter the cleft from inside the cell they at first move parallel to the z-axis. After some time, their motion turns from vertical to radial direction. Due to the ratio $h/R < 10^{-2}$ the cleft is considered as an infinite thin disk of radius R allowing only a radial motion. Therefore, the flux of K^+ ions into the cleft during electrical excitation is described by a positive constant source term[16] $\lambda_{K^+} = 11$ pA $\mu\mathrm{m}^{-3}$ independent of position and time. The source term for the other ions is zero resulting in $\lambda_{tot} = \lambda_{K^+}$ and $\zeta_{tot} = \lambda_{K^+}/e$.

For the analysis of the densities and the potential in the cleft polar coordinates (r, ϕ) are appropriate, meaning that there is no z-dependence because of the disk-shaped geometry. It is also assumed that there is no ϕ-dependence. One obtains with Eq. (6) for $\delta\rho_{tot}(r, t)$

$$\frac{\partial^2 \delta\rho_{tot}(r,t)}{\partial r^2} + \frac{1}{r}\frac{\partial \delta\rho_{tot}(r,t)}{\partial r} - \frac{1}{L_D^2}\delta\rho_{tot}(r,t) - \frac{1}{D}\frac{\partial \delta\rho_{tot}(r,t)}{\partial t} = -\frac{\lambda_{K^+}}{D}. \tag{14}$$

The boundary conditions are electroneutrality at $r = R$ and inside the cleft at $t = 0$, and the long term limit[16]

$$\begin{aligned} \delta\rho_{tot}(r,0) &= 0, \\ \delta\rho_{tot}(R,t) &= 0, \\ \lim_{t\to\infty} \delta\rho_{tot}(r,t) &= \frac{\lambda_{K^+} L_D^2}{D}\left(1 - \frac{I_0(r/L_D)}{I_0(R/L_D)}\right), \end{aligned} \tag{15}$$

with the Bessel function I_0.

By standard methods the solution can be given in the form of a Fourier-Bessel series

$$\delta\rho_{tot}(r,t) = \frac{2\lambda_{K^+} L_D^2}{D} S_1(r,t) \tag{16}$$

with

$$S_1(r,t) = \sum_{\nu=1}^{\infty} \frac{J_0\left(\frac{\gamma_\nu}{R} r\right)}{\left(1 + \frac{L_D^2}{R^2}\gamma_\nu^2\right)\gamma_\nu J_1(\gamma_\nu)} \left(1 - e^{-\frac{D}{L_D^2}\left(1 + \frac{L_D^2}{R^2}\gamma_\nu^2\right)t}\right). \tag{17}$$

J_0 and J_1 are the Bessel functions of zeroth and first order and γ_ν are the zeros of J_0 ordered by increasing value. Because $L_D^2/R^2 \approx 3 \times 10^{-9}$ the series can be approximated by an analytic function (see the Appendix). It follows

$$\delta\rho_{tot}(r,t) \approx \lambda_{K^+}\tau_c \left(1 - \frac{I_0(r/L_D)}{I_0(R/L_D)}\right)(1 - e^{-t/\tau_c}) \tag{18}$$

with the time constant $\tau_c = L_D^2/D$ which characterizes the time to reach a stationary total charge situation. With a diffusion coefficient $D = 2.0 \times 10^{-9}\ \mathrm{m}^2\ \mathrm{s}^{-1}$ one obtains $\tau_c = 0.32$ ns. Due to the exponential behaviour for large arguments of the Bessel function I_0, the r-dependent term $(1 - I_0(r/L_D)/I_0(R/L_D))$ is about 1. Only if $R - L_D < r \le R$, then the term decreases to zero like a stepfunction. Thus, considering a time larger than 1 ns the total charge density is almost constant

$$\delta\rho_{tot}(r,t) \approx \lambda_{K^+}\tau_c. \tag{19}$$

The ratio $(\lambda_{K^+}\tau_c)/(e(n^e_{K^+} + n^e_{Na^+}))$ provides some information on the increase in the positive charge inside the cleft. With the actual numbers, the ratio is $<10^{-9}$ which is quite close to electroneutrality.

From Eq. (8) it follows for $\delta n_{tot}(r, t)$

$$\frac{\partial^2 \delta n_{tot}(r,t)}{\partial r^2} + \frac{1}{r}\frac{\partial \delta n_{tot}(r,t)}{\partial r} - \frac{1}{D}\frac{\partial \delta n_{tot}(r,t)}{\partial t} = -\frac{\lambda_{K^+}}{eD}. \tag{20}$$

The boundary conditions are

$$\begin{aligned} \delta n_{tot}(r,0) &= 0, \\ \delta n_{tot}(R,t) &= 0, \\ \lim_{t\to\infty} \delta n_{tot}(r,t) &= \frac{\lambda_{K^+} R^2}{4eD}\left(1 - \frac{r^2}{R^2}\right). \end{aligned} \tag{21}$$

Again, the solution is expressed by a Fourier-Bessel series

$$\delta n_{tot}(r,t) = \frac{2\lambda_{K^+} R^2}{eD} S_2(r,t) \tag{22}$$

with

$$S_2(r,t) = \sum_{\nu=1}^{\infty} \frac{J_0\left(\frac{\gamma_\nu}{R} r\right)}{\gamma_\nu^3 J_1(\gamma_\nu)}(1 - e^{-\frac{D}{R^2}\gamma_\nu^2 t}). \tag{23}$$

Using the approximation (A7) (see the Appendix) it follows for $\delta n_{tot}(r, t)$

$$\delta n_{tot}(r,t) \approx \frac{\lambda_{K^+}\,\gamma_1^2\,\tau_g}{4e}\left(1 - \frac{r^2}{R^2}\right)(1 - e^{-t/\tau_g}) \tag{24}$$

with the geometry-dependent time constant $\tau_g = R^2/(D\gamma_1^2) = 20$ ms. In spite of the total charge density it takes much longer for the total ion density to reach the stationary state.

Applying the linear superposition (10) it follows for the single charge densities

$$\rho_{K^+}(r,t) = \rho^e_{K^+} - \frac{n^e_{K^+}}{n^e_{tot}}\overline{\delta\rho}(r,t) + \frac{2\lambda_{K^+} R^2}{D} S_2(r,t), \tag{25}$$

$$\rho_{Na^+}(r,t) = \rho^e_{Na^+} - \frac{n^e_{Na^+}}{n^e_{tot}}\overline{\delta\rho}(r,t), \tag{26}$$

$$\rho_{Cl^-}(r,t) = \rho^e_{Cl^-} - \frac{n^e_{Cl^-}}{n^e_{tot}}\overline{\delta\rho}(r,t), \tag{27}$$

with

$$\overline{\delta\rho}(r,t) = \frac{2\lambda_{K^+}R^2}{D}\left(S_2(r,t) - \frac{L_D^2}{R^2}S_1(r,t)\right). \tag{28}$$

Neglecting the term containing L_D^2/R^2 and using the approximation (A7) one finally calculates

$$\rho_i(r,t) \approx \rho^e_i + \alpha_i \delta n_{tot}(r,t) \tag{29}$$

with $\delta n_{tot}(r,t)$ given by Eq. (24) and

$$\alpha_{K^+} = e\left(1 - \frac{n^e_{K^+}}{n^e_{tot}}\right), \tag{30}$$

$$\alpha_{Na^+} = -e\frac{n^e_{Na^+}}{n^e_{tot}}, \quad \alpha_{Cl^-} = -e\frac{n^e_{Cl^-}}{n^e_{tot}}. \tag{31}$$

Using the numbers given above one has $\alpha_{K^+} = 0.98\ e$, $\alpha_{Na^+} = -0.48\ e$, and $\alpha_{Cl^-} = -0.50\ e$. In contrast to the total charge density's dependence on the time constant τ_c, it can be seen from Eq. (29) that the time dependence of the single charge densities is identical to that of the total ion density, characterized by τ_g. In Fig. 2, the changes $\delta\rho_i(r,t) = \alpha_i\delta n_{tot}(r,t)$ for the three ion species are plotted as a function of r/R and for the stationary state $t > 200$ ms. It shows that the K^+ ions accumulate inside the cleft mainly at the center. Cl^- ions will accumulate at a lower level, while the amount of Na^+ ions decreases. In Fig. 3, the normalized transient profile for three times (2, 20, and 200 ms) is plotted.

It should be noted that the L_D^2/R^2-dependent term in Eq. (28) cannot be neglected if summing up $\Sigma\rho_i$ to get ρ_{tot}. In this case, the exact formulae (25)–(28) have to be used because the leading terms cancel out.

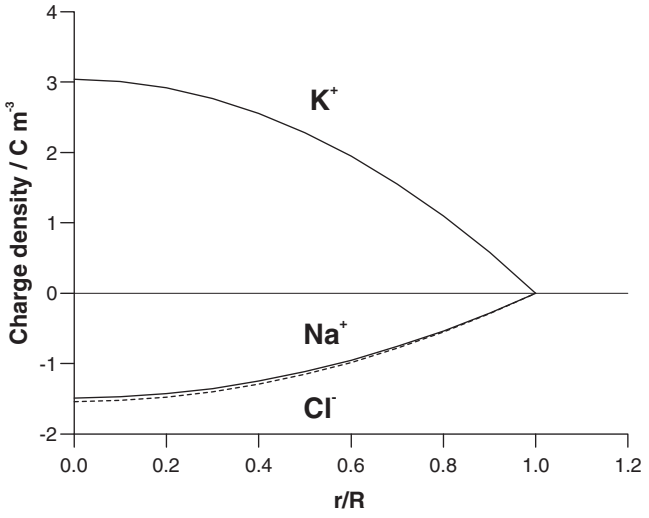

FIG. 2. The parabolic change of the single charge densities $\delta_i(r,\ t) = \alpha_i\delta n_{tot}(r,t)$ as a function of r/R for the stationary state ($t > 200$ ms). $\delta n_{tot}(r,t)$ is calculated by using Eq. (24).

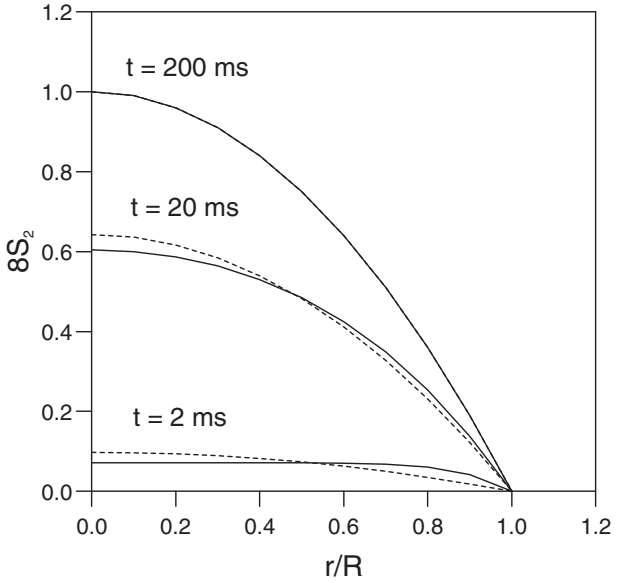

FIG. 3. The function $8 \cdot S_2$ as a function of r/R for the times t = 2, 20, and 200 ms. The solid lines show the analytical function of Eq. (A7), the dashed lines correspond to the summation of Eq. (23) with an error less than 10^{-3}. For $t > 200$ ms, the difference between the analytical formula and the summation is not visible.

When $\delta\rho_{tot}$ is known the potential $\psi(r,t)$ can be calculated by integrating the Poisson equation

$$\frac{1}{r}\frac{\partial}{\partial r}\left(r\frac{\partial\psi(r,t)}{\partial r}\right) = -\frac{2\lambda_{K^+}L_D^2}{\epsilon_0\epsilon_r D} \times \sum_{\nu=1}^{\infty}\frac{J_0\left(\frac{\gamma_\nu}{R}r\right)}{\left(1+\frac{L_D^2}{R^2}\gamma_\nu^2\right)\gamma_\nu J_1(\gamma_\nu)} \times\left(1 - e^{-\frac{D}{L_D^2}\left(1+\frac{L_D^2}{R^2}\gamma_\nu\right)t}\right). \tag{32}$$

With the boundary conditions of $\psi(0,t)$ having no pole and $\psi(R,t) = 0$, direct integration gives

$$\psi(r,t) = \frac{2\lambda_{K^+}L_D^2R^2}{\epsilon_0\epsilon_r D} \times \sum_{\nu=1}^{\infty}\frac{J_0\left(\frac{\gamma_\nu}{R}r\right)}{\left(1+\frac{L_D^2}{R^2}\gamma_\nu^2\right)\gamma_\nu^3 J_1(\gamma_\nu)}\left(1 - e^{-\frac{D}{L_D^2}\left(1+\frac{L_D^2}{R^2}\gamma_\nu^2\right)t}\right). \tag{33}$$

Using some algebra $\psi(r,t)$ can be written as

$$\psi(r,t) = \frac{2\lambda_{K^+}L_D^2R^2}{\epsilon_0\epsilon_r D}\left(S_3(r,t) - \frac{L_D^2}{R^2}S_1(r,t)\right) \tag{34}$$

with

$$S_3(r,t) = \sum_{\nu=1}^{\infty}\frac{J_0\left(\frac{\gamma_\nu}{R}r\right)}{\gamma_\nu^3 J_1(\gamma_\nu)}\left(1 - e^{-\frac{D}{L_D^2}\left(1+\frac{L_D^2}{R^2}\gamma_\nu^2\right)t}\right). \tag{35}$$

Again, by neglecting the terms containing L_D^2/R^2 the potential is simplified. Unlike Eq. (18), Eq. (36) contains only

elementary functions. One obtains

$$\psi(r,t) = \frac{\lambda_{K^+} R^2 \tau_c}{4\epsilon_0 \epsilon_r} \left(1 - \frac{r^2}{R^2}\right)\left(1 - e^{-\frac{t}{\tau_c}}\right) \tag{36}$$

with the same time constant τ_c as for $\delta\rho_{tot}(r, t)$.

The potential and all the densities show a linear dependence on the source term λ_{K^+}. If all the membrane channels stay closed, the state is characterized by $\lambda_{K^+} = 0$ and it follows that the potential and the densities do not change, maintaining the equilibrium values.

The above calculations are received for a cleft which is represented by a infinitely thin disk. Therefore, it is worthwhile to comment on the situation when the finite thickness of $h \approx 100$ nm of the cleft is considered. In that case, it takes a certain time for the K^+ ions to cross the cleft from the top to the bottom before filling the whole cleft. An appropriate time constant for this process could be defined by $\tau_h = h^2/D \approx 5$ μs. As a result, the assumption of a constant λ_{K^+} inside the cleft would be realistic only after a time of several τ_h. After that time the total charge density $\delta\rho_{tot}$ is constant and the potential ψ is a time independent parabolic function in the radial direction. This time period is still several orders of magnitude smaller than the transient time τ_g.

IV. SUMMARY

The Poisson-Nernst-Planck equations (1)–(3) have been linearized and decoupled. The system has been transformed into Eqs. (6), (8), and (13) for the quantities $\delta\rho_{tot}(\boldsymbol{r}, t)$, $\delta n_{tot}(\boldsymbol{r}, t)$, and $\psi(\boldsymbol{r}, t)$, respectively. Each of the equations can be solved by standard methods depending on the geometry and the boundary conditions. The single charge densities are expressed by a linear superposition of $\delta n_{tot}(\boldsymbol{r}, t)$ and $\delta\rho_{tot}(\boldsymbol{r}, t)$.

The method was applied to the cleft between an electrically excited cell and a FET. The cleft was represented by a radially symmetric disk. Assuming a constant influx of K^+ ions into the cleft, the charge densities and the potential were exactly calculated and represented by Fourier-Bessel series. Using the fact that the ratio L_D^2/R^2 is on the order of 10^{-9}, the series can approximated by analytical functions.

The system is characterized by the two time constants $\tau_c = L_D^2/D$ and $\tau_g = R^2/(D\gamma_1^2)$. If the cleft is represented by an infinitely thin disk, the total charge density $\delta\rho_{tot}(r, t)$ depends on τ_c (Eq. (18)), and it is shown that after a nanosecond $\delta\rho_{tot}(r, t)$ is constant inside the cleft, independent of position and time (Eq. (19)). From Poisson's equation it follows that the potential is parabolic with the same time dependence (Eq. (36)). If a finite thickness, $h \approx 100$ nm, of the cleft is assumed, the situation is delayed and characterized by a time constant $\tau_h = h^2/D$, which is on the order of some microseconds. The transient state of the total ion density $\delta n_{tot}(r, t)$ (Eq. (24)) and the single ion charge densities $\delta\rho_i(r, t)$ (Eq. (29)) takes much longer. It is given by the time constant τ_g, which is in the range of 100 ms. This leads to the following interpretation of the time dependent situation inside the cleft: when the membrane channels open, K^+ ions enter the cleft increasing the positive charge there. As a consequence, some other positive ions leave the cleft through its outer boundary. Due to the ratio $n^e_{Na^+}/n^e_{K^+} = 28$, mainly Na^+ ions leave the cleft. In addition, some negative Cl^- ions will be attracted by the increased positive charge and enter the cleft through the outer boundary. The resulting effective total charge $\delta\rho_{tot}(r, t)$ reaches the stationary state in less than 100 μs. However, the flux of different ion species will continue much longer up to the order of τ_g. After some 100 ms the final stationary state is reached with no flux of Na^+ or Cl^- ions because the electrical field and the concentration gradients are balanced. Only K^+ ions leave the cleft continuously through the outer boundary in the same amount that they enter the cleft via the membrane channels.

APPENDIX: SOME PROPERTIES OF S_1, S_2, AND S_3

With the following analytical relations the series S_1, S_2, and S_3 can be simplified:[17,18]

$$1 = 2\sum_{\nu=1}^{\infty} \frac{J_0\left(\frac{\gamma_\nu}{R} r\right)}{\gamma_\nu J_1(\gamma_\nu)}, \tag{A1}$$

$$1 - \frac{r^2}{R^2} = 8\sum_{\nu=1}^{\infty} \frac{J_0\left(\frac{\gamma_\nu}{R} r\right)}{\gamma_\nu^3 J_1(\gamma_\nu)}, \tag{A2}$$

$$\frac{I_0(r/L_D)}{I_0(R/L_D)} = 2\sum_{\nu=1}^{\infty} \frac{\gamma_\nu J_0\left(\frac{\gamma_\nu}{R} r\right)}{\left(\gamma_\nu^2 + \frac{R^2}{L_D^2}\right) J_1(\gamma_\nu)}. \tag{A3}$$

From Eqs. (A1) and (A3), it follows

$$1 - \frac{I_0(r/L_D)}{I_0(R/L_D)} = 2\sum_{\nu=1}^{\infty} \frac{J_0\left(\frac{\gamma_\nu}{R} r\right)}{\gamma_\nu \left(1 + \frac{L_D^2}{R^2}\gamma_\nu^2\right) J_1(\gamma_\nu)}. \tag{A4}$$

Equations (A1)–(A4) are valid for $0 \le r/R < 1$, in addition Eqs. (A2) and (A4) also for $r/R = 1$.

The series S_1 and S_3 include the exponential terms $\exp(-\frac{D}{L_D^2}(1 + \frac{L_D^2}{R^2}\gamma_\nu^2)t$. With $L_D^2/R^2 \approx 3 \times 10^{-9}$ the term $\frac{L_D^2}{R^2}\gamma_\nu^2$ is negligible for $\nu \ll 10^4$, the major part of the series.

One then obtains

$$S_1(r,t) \approx \frac{1}{2}\left(1 - \frac{I_0(r/L_D)}{I_0(R/L_D)}\right)\left(1 - e^{-\frac{D}{L_D^2}t}\right) \tag{A5}$$

and

$$S_3(r,t) \approx \frac{1}{8}\left(1 - \frac{r^2}{R^2}\right)\left(1 - e^{-\frac{D}{L_D^2}t}\right). \tag{A6}$$

The above conclusion is not possible for S_2 which contains the exponential term $\exp(-D\gamma_\nu^2 t/R^2)$. However, a replacement of S_2 by

$$S_2(r,t) \approx \frac{1}{8}\left(1 - \frac{r^2}{R^2}\right)\left(1 - e^{-\frac{D}{R^2}\gamma_1^2 t}\right) \tag{A7}$$

is useful in the sense of maintaining the boundary conditions and characterizing the functional behaviour. The quantity γ_1 is the first zero of J_0. A comparison between the analytical function (A7) and the numerical summation of Eq. (23) is shown in Fig. 3.

The series S_1, S_2, and S_3 were also evaluated numerically to compare them with the corresponding analytical approximations. The series S_1 converges very slowly while S_2 and S_3 converge much faster. The Bessel functions J_0 and J_1 are usually part of the standard mathematical software programs. The low order zeros of J_0 were directly programmed, while for large order zeros McMahon's expansion was used.[19] For different values $0 \leq r/R \leq 1$ and the times $t = 0.03$, 0.3, 3 ns, the upper summation index N is about 3000 with an absolute maximum error $<10^{-2}$ for S_1. It should be noted that the large index is related to $r/R = 0$ with $J_0(0) = 1$. For the values $r/R \neq 0$, the function $J_0(\gamma_\nu r/R)$ changes sign as a function of increasing ν and the coefficients of the series partly cancel out. By keeping an equal error N could be reduced to about 100. As a result of the numerical calculations, it could be seen that the series S_1 oscillates around the function (A5) for an increasing summation index showing that (A5) is a good approximation. The series S_3 converges much faster resulting in an index $N = 13$ for the same values of r/R and t though for a lower error 10^{-3}. Again, it turned out that the function (A6) is a good approximation of the series S_3. The series S_2 was tested for the same r/R values but for the transient times $t = 2$, 20, 200 ms. In connection with an error of $<10^{-3}$, an index $N \approx 20$ was obtained for S_2.

[1] J. W. Jerome, *Analysis of Charge Transport - A Mathematical Study of Semiconductor Devices* (Springer-Verlag, 1996).
[2] S. Selberherr, *Analysis and Simulation of Semiconductor Devices* (Springer-Verlag, 1984).
[3] M. Z. Bazant, Phys. Rev. E **70**, 021506 (2004).
[4] R. S. Eisenberg, J. Membr. Biol. **150**, 1 (1996).
[5] M. G. Kurnikova, R. D. Coalson, P. Graf, and A. Nitzan, Biophys. J. **76**, 642 (1999).
[6] B. Corry, S. Kuyucak, and S. H. Chung, J. Gen. Physiol. **114**, 597 (1999).
[7] N. Tankovsky and E. Syrakov, J. Phys.: Condens. Matter **17**, 1225 (2005).
[8] J. Pods, J. Schönke, and P. Bastian, Biophys. J. **105**, 242 (2013).
[9] J. Jasielec, R. Filipek, K. Szyszkiewicz, J. Fausek, M. Danielewski, and A. Lewenstam, Comput. Mater. Sci. **63**, 75 (2012).
[10] Y. Shinagawa, J. Theor. Biol. **72**, 603 (1978).
[11] G. V. Bicknell, H. G. L. Coster, and E. P. George, Bioelectrochem. Bioenergetics **4**, 298 (1977).
[12] A. Golovnev and S. Trimper, Phys. Lett. A **374**, 2886 (2010).
[13] J. Schönke, J. Phys. A **45**, 455204 (2012).
[14] A. Golovnev and S. Trimper, J. Chem. Phys. **134**, 154902 (2011).
[15] P. Debye and H. Falkenhagen, Phys. Z. **29**, 139 (1928).
[16] M. Pabst, G. Wrobel, F. Sommerhage, and A. Offenhäusser, Eur. Phys. J. E **24**, 1 (2007).
[17] F. Bowman, *Introduction to Bessel Functions* (Dover Publications, 1958).
[18] *Higher Transcendental Functions*, edited by A. Erdélyi (McGraw-Hill, 1953), Vol. II.
[19] *Handbook of Mathematical Functions*, edited by M. Abramowitz and I. Segun (Dover Publications, 1968).